Supporting Information

# Crystal Photonics Foundry: Geometrical Shaping of Molecular Single Crystals into Next Generation Optical Cavities

Vuppu Vinay Pradeep, Melchi Chosenyah, Evgeniy Mamonov,* Rajadurai Chandrasekar*

V. V. Pradeep, M. Chosenyah, Prof. R. Chandrasekar
School of Chemistry and Centre for Nanotechnology, University of Hyderabad,
Prof. C. R. Rao Road, Gachibowli, Hyderabad 50046, India
E-mail: *r.chandrasekar@uohyd.ac.in*

Dr. E. Mamonov
Department of Physics, Quantum Electronics Division, Moscow State University
Moscow 119991, Russia
E-mail: *mamonov@shg.ru*

Table of Contents:

## 1. Materials:

Perylene, Coumarin-153, potasium iodide, iodine and sodium cyanide were purchased from commercial suppliers. HPLC solvents were used for self-assembly.

## 2. Preparation of microcrystals:

**2.1. Perylene microcrystals:** Bottom-up method was used to naturally grow α-form perylene microcrystals on a clean coverslip. Tetrahydrofuran (HPLC grade) solution of perylene (1 mg/1 mL, 4 mM) was used to fabricate microcrystals. The solution was sonicated for 30 s and kept for 5 min without any disturbance. Later, 2-3 drops (≈20 μl) of perylene solution was drop-casted on the clean glass coverslip and allowed to evaporate. The solvent evaporation allowed growth of numerous square- and rectangular-shaped microcrystals of various sizes (Figure S1a).

**2.2. Coumarin-153 microcrystals:** Ambient pressure vapor deposition technique was used to prepare coumarin-153 microcrystals. For this <1 mg of the compound was placed on a clean coverslip. Later, another coverslip was placed on it using two supporting stubs of height (Δh) 1 mm. The whole setup was placed on a hot plate and heated slowly up to 110 $^{o}$C. It was allowed to sublime at 110 $^{o}$C for about a minute. Then, the sample was slowly cooled down to room temperature to obtain numerous microcrystals on the top coverslip (Figure S1b).

## 3. Instrumentation methods:

### 3.1. Polarised light microscope:

The images of fabricated and milled microcrystals were captured using a NIKON eclipse LV100N POL polarising microscope. It was equipped with an epi-illuminator (NIKON 12V 50W), DS-Fi3 camera having a 5.9 megapixel CMOS sensor, which enables superior color reproduction and NIKON TU plan fluor EPI P series objectives (4×, 10×, 20× and 50×) for pin-sharp aberration-free images regardless of magnification.

### 3.2. Atomic force microscope (AFM):

All the AFM experiments were carried out on an Oxford Asylum Research MFP-3D Origin. The image processing was carried out by using AR 16.25.226 software provided by the manufacturer. The images were recorded in a contact mode topography using a silicon cantilever (NSG 10_DLC) with a diamond-like carbon tip (NT-MDT). The dimension of the tip is

as follows: cantilever length = 100 (±5) µm, cantilever width = 35 (±3) µm, cantilever thickness = 1.7–2.3 µm, resonance frequency = 190–325 kHz, force constant = 5.5–22.5 N/m, tip height = 10–20 nm.

**3.3. Field Emission Scanning Electron Microscopy (FESEM):**

A thin layer of gold was coated on the substrate using a 15 µA current for 80 sec. The size and morphology of the milled coumarin-153 microcrystals were examined by using a Zeiss field emission scanning electron microscope operating at an accelerating voltage of 5 kV.

**3.4. Focused Ion Beam (FIB) milling:**

For the FIB milling of microcrystals, thermo scientific SCIOS 2 dual-beam instrument was used. Initially, the microcrystals were imaged in SEM mode with a 0.0° tilt angle, 0.4 nA beam current and an accelerating beam voltage of 5.00 kV. Later, the sample was tilted 52° to align orthogonal to FIB (Gallium ion source). Using pre-defined shapes in the software (in this case rectangular and circular shapes), the milling portions were selected. Then, 30 kV accelerating beam voltage and 0.1 nA probe current were applied to mill the microcrystals to desired shapes. The graphical representations of FIB milling of perylene, and coumarin-153 microcrystals are shown in Figure S3a, S5a, S6a. The shaded regions are the milling areas. Figure S3b, S5b, S6b show the sequence of photographs taken in iPhone 13 during crystal milling.

## 4. Fabrication of microstructures and photonic studies

Fluorescence spectra of the microcrystals were recorded on a Wi-Tec confocal spectrometer equipped with a Peltier-cooled CCD detector. Using 300 grooves/mm grating BLZ = 750 nm. All measurements were performed in transmission mode geometry with a 60x objective. A solid-state continuous-wave 405 nm laser was used as an excitation source. To collect the output signals from the specific area of microcrystals, 150× objective (N. A.: 0.95) was used. For acquiring a single spectrum before FIB milling, the laser power, integration time and accumulations were optimized to 0.05 mW, 0.5 s and 10, respectively. The images were processed by using Wi-Tec 5.2 software

**4.1. Fabrication of three different-sized microdiscs in a perylene microcrystal:** A single microcrystal was broken into pieces using an AFM cantilever tip. Later, FIB milling was carried out on the broken crystal to fabricate three microdiscs of diameters 3.88, 4.83, and 5.74 µm. The acceleration voltage and probe current was set to 30 kV and 100 pA. The microdiscs were

excited with a 405 nm continuous-wave laser in transmission mode geometry with an input power of 0.1 mW (objective: 60x) and the FL spectra were collected using the 150x objective having a numerical aperture of 0.95 (Figure S2).

**4.2. Fabrication of ring-shaped perylene microcrystal:** A single microcrystal of dimensions ≈ 8.4×8.17 $\mu m^2$ was selected. Later the crystal was milled into a ring-shaped crystal of diameters (outer and inner) 6.3 μm and 2.35 μm using a focused gallium ion beam of acceleration voltage 30 kV and a probe current of 100 pA. The fabricated ring-shaped microcrystal was subjected to a continuous-wave 405 nm laser in transmission mode geometry with an input power of 0.5 mW. The spectrum was collected with an integration time of 1.0 s and 20 accumulations (Figure S3).

**4.3. Fabrication of larger disc-shaped coumarin-153 microcrystal:** A single microcrystal of dimensions ≈ 9.4×9.8 $\mu m^2$ was selected. The single-crystal microspectroscopic studies revealed the FP-type resonator behavior with an FSR of 3.81 nm. The inset of figure S6b shows the AFM height profile of the crystal which is found to be 1.18 μm. A focused gallium ion beam with an acceleration voltage of 30 kV and a probe current of 100 pA was used to mill the crystal into a disc-shaped crystal with a diameter of 7.47 μm. An input power of 0.3 mW was applied to the fabricated disc-shaped microcrystal and the spectra were recorded with an integration time of 0.5 s and 10 accumulations (Figure S5).

**4.4. Fabrication of rectangular-shaped coumarin-153 microcrystal:** A single microcrystal dimension ≈ 8.3×9.9 $\mu m^2$ was selected. The single-crystal microspectroscopic studies revealed the FP-type resonator behavior with an FSR of 4.07 nm. The inset of figure S8b shows the AFM height profile of the crystal which is found to be 0.91 μm. A focused gallium ion beam with an acceleration voltage of 30 kV and a probe current of 100 pA was used to mill the crystal into a rectangular-shaped crystal with dimensions 6.3×5.5 $\mu m^2$. An input power of 0.5 mW was applied to the fabricated disc-shaped microcrystal and the spectra were recorded with an integration time of 0.5 s and 10 accumulations (Figure S6).

**4.5. Fabrication of smaller disc-shaped coumarin 153 microcrystal:** A single microcrystal of dimensions ≈ 9.1×11.1 $\mu m^2$ was selected. The single-crystal micro-spectroscopic studies revealed crystal's FP-type resonance with an FSR of 4.8 nm. The inset of figure S7b shows the AFM height profile of the crystal which is found to be 1.33 μm. Later, the crystal was milled into a disc-shaped crystal of diameters 2.5 μm using a focused gallium ion beam of acceleration voltage 30 kV and a probe current of 100 pA. The fabricated disc-shaped

microcrystal was excited with a continuous-wave 405 nm laser with an input power of 0.5 mW. The FL spectra were collected with an integration time of 0.5 s and for 10 accumulations (Figure S7).

## 5. Post-processing techniques

There are two methods incorporated to remove gold coating from the molecular crystals and the substrate.

**5.1. Washing with Lugol's Iodine solution (method 1):** The Lugol's iodine solution was prepared using 10g of potassium iodide, 5 g of iodine and 100 mL of distilled water. Later, FIB milled microcrystals containing coverslip was placed in a petridish. The freshly prepared solution was added gently via the walls of the petridish. The coverslip was allowed to soak for about 1-2 minutes, then the solution was pipetted out using a dropper. Later, it was washed with distilled water.

**5.2. Exposure to HCN vapors (method 2):** 1 g of NaCN was placed on the tissue paper and made a packet of it. Later, the packet was placed in the glass container, and a cardboard having 2 holes was placed over it. Now, the gold-coated coverslip (FIB milled microcrystals containing coverslip) was gently placed on the cardboard. Finally, 3-4 drops of water were added through the holes of the cardboard and the glass container was closed using the lid and tightly sealed using parafilm tape (Figure S3). The added water droplets react with NaCN, which in turn results in the generation of HCN vapors. These vapors slowly react with the gold layer on the coverslip. Within a day, the gold layer was completely reacted with HCN and the formed AuCN was settled on the coverslip. Finally, the gold-layer free coverslip was obtained after washing with distilled water (Figure S4).

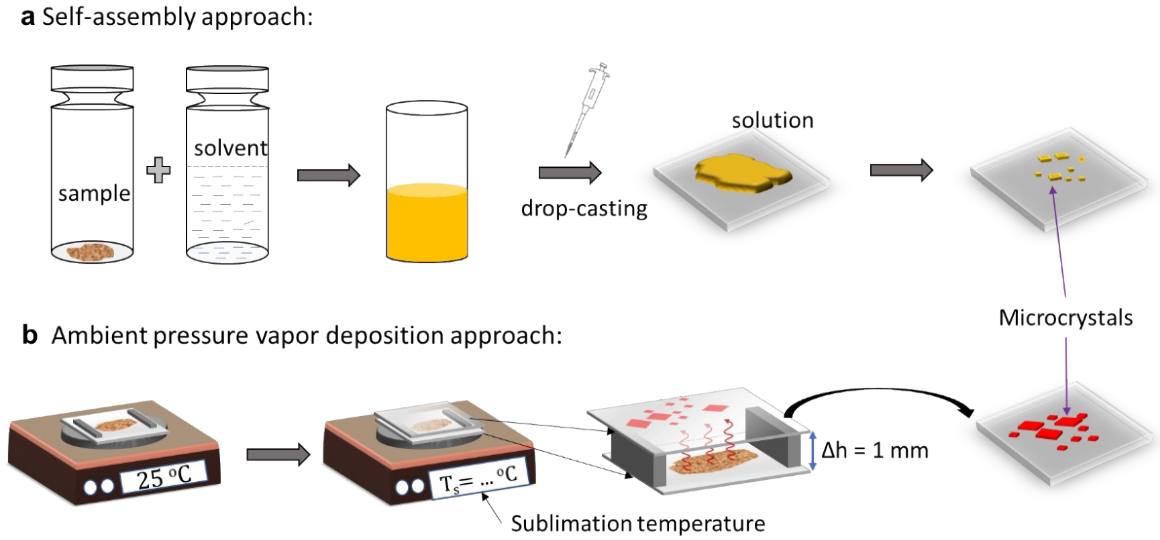


**Figure S1:** a,b) Schematic representation of self-assembly and ambient pressure vapor deposition techniques, respectively to grow microcrystals of an organic compound.

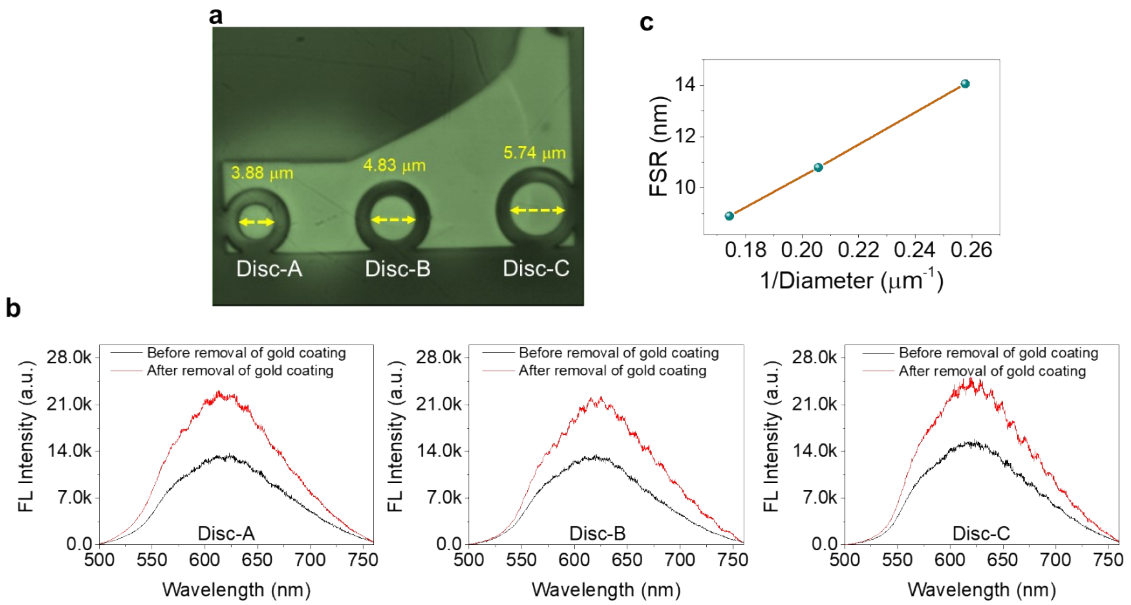


**Figure S2:** a) Confocal image of different-sized microdiscs (Disc-A, Disc-B and Disc-C) milled on a broken perylene single crystal using FIB. b) The corresponding FL spectra before and after removal of gold coating. c) The plot of FSR vs 1/diameter shows the linear dependency of FSR on the diameter of the fabricated Disc-A to -C.

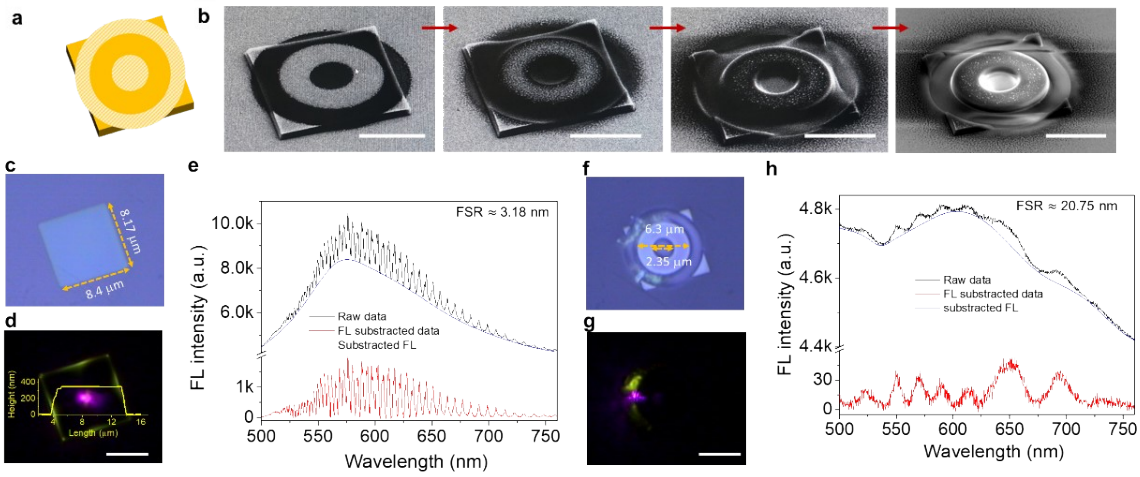


**Figure S3:** . a) The schematic of FIB milling of perylene. The shaded regions were milled using FIB. b) The corresponding series of photographs taken in iPhone-13 during milling. Scale bar 4 µm. c and f) Optical microscopic d and g) FL images of a square-shaped perylene single crystal and a ring-shaped crystal, respectively. e and h) The spectra showing the FL raw data (black), background-subtraction data (blue) and the substracted FL data (optical resonances, red) of the square-shaped perylene single crystal and a ring-shaped crystal, respectively. Scale bar 5 µm.

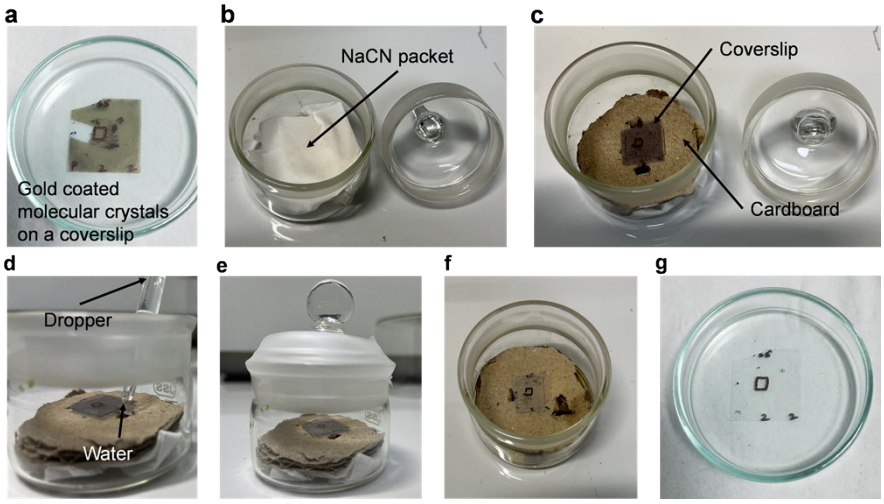


**Figure S4:** Photographic images of a) gold coated coverslip containing molecular crystals in a petridish, b,c) NaCN packet and cardboard containing holes in a container, respectively. d) Addition of water droplets through the holes of the cardboard. e,f) Photographic images of the sealed (while reacting) and open container (after reaction), respectively. g) Washing of coverslip in a petridish with distilled water.

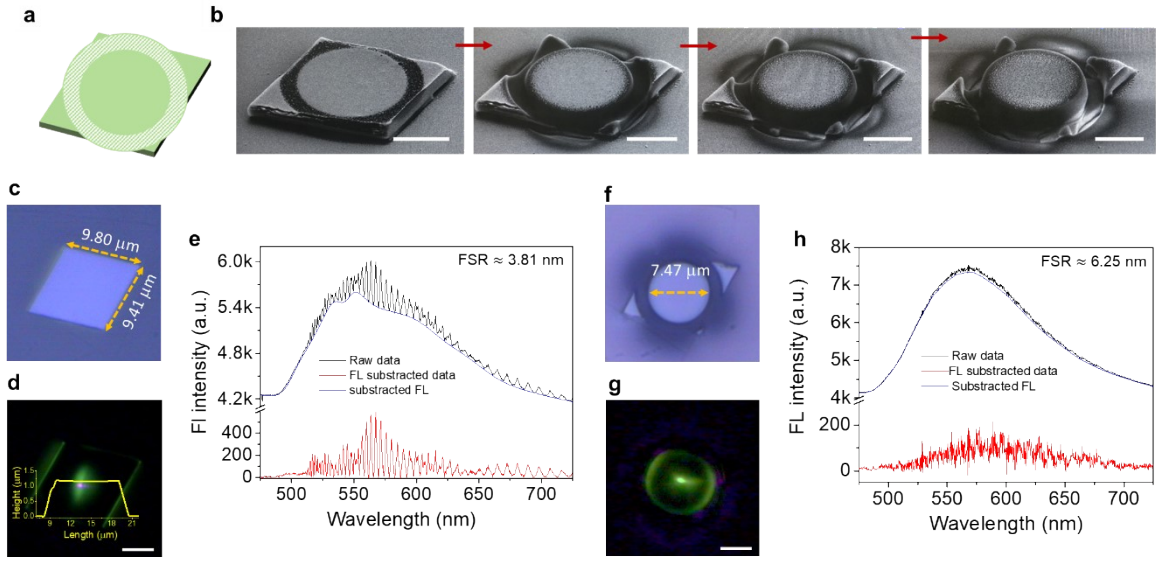


**Figure S5:** a) Schematic of bitmap showing the milling pattern. b) The series of photographs taken in iPhone-13 during milling. Scale bar 4 µm. c,f) Optical microscopic d,g) FL images of rhombus shaped coumarin-153 single crystal (before milling) and disc-shaped crystal (after milling), respectively. e,h) The spectra showing the FL raw data (black), background-subtraction data (blue) and the substracted FL data (optical resonances, red) of coumarin single crystal before and after milling to disc-shaped crystal, respectively. Scale bar 4 µm.

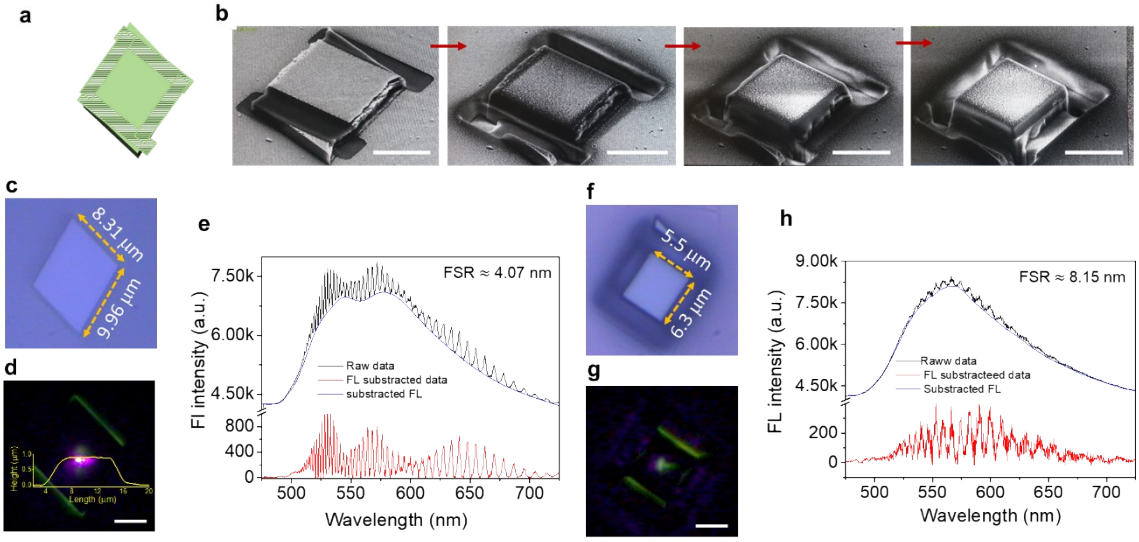


**Figure S6:** a) Schematic of bitmap showing the milling pattern. b) The corresponding series of photographs taken in iPhone-13 during milling. Scale bar 4 µm. c and f) Optical microscopic, d,g) FL images of rhombus shaped coumarin 153 single crystal (before milling) and rectangular-shaped crystal (after milling), respectively. e,h) The spectra showing the FL raw data (black), background-subtraction data (blue) and the substracted FL data (optical resonances, red) of coumarin single crystal before and after milling to rectangular-shaped crystal, respectively. Scale bar 4 µm.

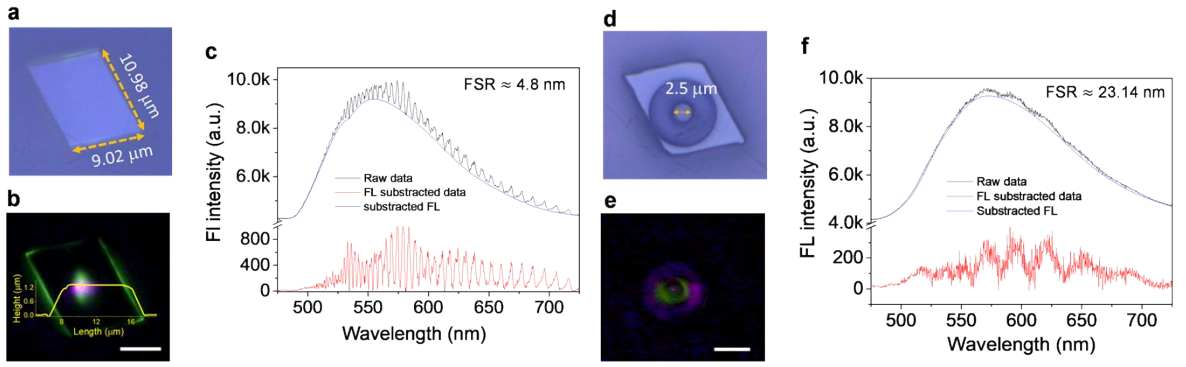


**Figure S7:** a,d) Optical microscopic b,e) FL images of coumarin 153 single crystal (before milling) and disc-shaped crystal (after milling), respectively. c,f) The spectra showing the FL raw data (black), background-subtraction data (blue) and the substracted FL data (optical resonances, red) of coumarin single crystal before and after milling to disc-shaped crystal, respectively. Scale bar 5 µm.

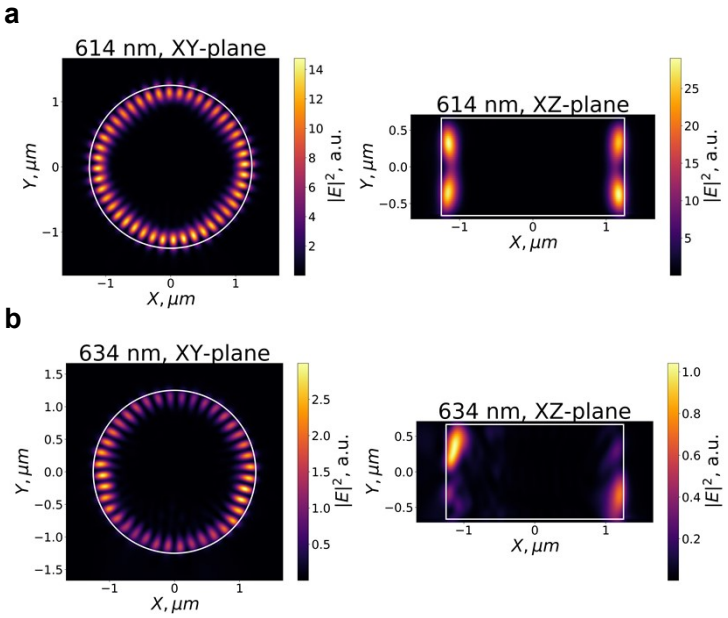


**Figure S8:** a,b) Electric field distributions in 2.5 µm microresonator at wavelengths of 614 nm and 634 nm (top and bottom), respectively. Left pictures are field distribution cross-sections parallel to the substrate plane located at half of resonator's height above the substrate, right pictures are cross-sections perendicular to the substrate. White lines denote resonator borders.